

# *DFT study of ligand binding in the $\beta$ 1 adrenergic receptor*

Article

Accepted Version

Safarian, D., Simons, M., Evans, R. G., Peterson, L. W. and Cafiero, M. ORCID: <https://orcid.org/0000-0002-4895-1783> (2021) DFT study of ligand binding in the  $\beta$ 1 adrenergic receptor. Computational and Theoretical Chemistry, 1199. 113208. ISSN 2210271X doi: 10.1016/j.comptc.2021.113208 Available at <https://centaur.reading.ac.uk/108191/>

It is advisable to refer to the publisher's version if you intend to cite from the work. See [Guidance on citing](#).

Published version at: <http://www.scopus.com/inward/record.url?eid=2-s2.0-85102896960&partnerID=MN8TOARS>

To link to this article DOI: <http://dx.doi.org/10.1016/j.comptc.2021.113208>

Publisher: Elsevier

All outputs in CentAUR are protected by Intellectual Property Rights law, including copyright law. Copyright and IPR is retained by the creators or other copyright holders. Terms and conditions for use of this material are defined in the [End User Agreement](#).

[www.reading.ac.uk/centaur](http://www.reading.ac.uk/centaur)

**CentAUR**

Central Archive at the University of Reading

Reading's research outputs online

# DFT study of ligand binding in the $\beta_1$ adrenergic receptor

Daryna Safarian<sup>1</sup>, Megan Simons<sup>2</sup>, Rebecca G. Evans<sup>3</sup>, Larry Peterson<sup>1</sup>, Mauricio Cafiero<sup>4</sup>

<sup>1</sup>*Rhodes College, 2000 North Parkway Memphis, TN 38112,*

<sup>2</sup>*Southern Methodist University, Texas, USA*

<sup>3</sup>*Princeton University, New Jersey, USA*

<sup>4</sup>*University of Wolverhampton, Wulfruna St., Wolverhampton, U.K.*

## Abstract

The  $\beta_2$ -adrenergic receptor, located in the prostate region, binds noradrenaline and can influence the growth of prostate tumors. The removal of *Adrb2*, the gene for this receptor, can halt tumor growth and thus can serve as an alternative to chemotherapy for cancer treatment. Inhibition of the receptor may have similar effects. Comparison of  $\beta_2$ - (PDB ID: 5X7D) and  $\beta_1$ -adrenergic receptor (PDB ID: 2Y04) structures showed a conserved binding region on Chain A offset by approximately eight amino acids between the two receptors. The structure of the  $\beta_1$ -adrenergic receptor with the bound partial agonist salbutamol was used to create a model of the active site of the  $\beta_2$ -adrenergic receptor. Potential inhibitors were optimized in the receptor binding site using M062X/6-31G with relaxed amino acid sidechains. Interaction energies between the ligands and the receptor were calculated using M062X/6-311+G\*. Positively charged inhibitors show greater interaction energies as compared to negatively charged inhibitors.

## 1. Introduction

In the western world, prostate carcinoma is the most prevalent malignancy in men [1]. Hormone therapy is currently the most common treatment. Androgen suppression therapy has been established as an accepted hormonal treatment for prostate cancer [2, p. 2]. While this is initially effective, after a while, tumors become resistant to hormonal treatment and develop into more aggressive types of prostate cancer. What remains as the biggest therapeutic challenge is its progression to castration resistant prostate cancer (CRPC) [3][4].

Prostate cancer results from the activation of the angiogenic switch, which induces exponential tumor growth. The angiogenic switch is a state in which pro-angiogenic factors dominate over anti-angiogenic signals; this includes the vascular endothelial growth and other secreted angiocrine factors [5][6]. It has been shown that nerves

play an active role in tumorigenesis and the further development of tumors by associating with blood vessels [5].  $\beta$ -Adrenergic receptors ( $\beta$ ARs) are part of the sympathetic nervous system; adrenergic signals delivered by sympathetic nerve fibers act on  $\beta$ ARs in the tumor microenvironment [5][7].  $\beta$ -Adrenergic signaling was found to be involved in the regulation of apoptosis, angiogenesis, neuroendocrine differentiation, migration, and metastasis of prostate cancer cells, and it is critical for the activation of the angiogenic switch, which promotes exponential tumor growth [5][8]. Lehrer and Rheinstein conducted a study examining the relationship of gene expression of *Adrb1* and *Adrb2* (encode  $\beta_1$ AR and  $\beta_2$ AR, respectively) with the gene expression of Forkhead box protein A1 (FOXA1), which regulates androgen receptor signaling and is a major contributor to prostate cancer development [9][10]. It was found that there is a correlation between alteration in these three genes, suggesting they work together to promote prostate tumor growth [10]. In the prostate,  $\beta_2$ AR is the dominating receptor in luminal cells, and it is responsible for over 95% of  $\beta$ AR binding activity [7].  $\beta_2$ AR is a seven-transmembrane G-protein coupled receptor activated by catecholamines (specifically adrenaline and noradrenaline), and acting through the cyclic-AMP (cAMP) signaling pathway, which activates cAMP dependent protein kinase (PKA) resulting in the development of aggressive prostate cancer [7][11]. Recent studies have shown that the repression of  $\beta_2$ AR with  $\beta$ -blockers has led to reduced prostate cancer mortality [2][5][7][8][10]. Inhibition of  $\beta_2$ AR signaling has the effect of delaying or preventing the domination of pro-angiogenic factors that promote tumor progression, positively affecting the obstruction of exponential tumor growth. Chan et al. studied the impacts that agonists, antagonists, and inverse agonists had on  $\beta_2$ AR and discuss common features among each class of studied ligands. The agonists that were studied have an aromatic ring connected to an ethanolamine backbone and the antagonists and inverse agonists studied have an oxymethylene bridge connecting the aromatic ring and ethanolamine backbone [12]. However, an important ligand for the development of  $\beta$  blockers, pronethalol, does not have the characteristic oxymethylene bridge [12], and this study is focused on testing a larger variety of ligands with different features.

The structure of  $\beta_2$ AR from the Protein Data Bank is bound to an antagonist, which blocks the active site; therefore,  $\beta_1$ AR was used as a model for  $\beta_2$ AR with an offset of the binding on Chain A. It was previously shown that clinically used  $\beta$ -blockers have little selectivity between  $\beta_1$ AR and  $\beta_2$ AR [13]. The focus of this work was to investigate a variety of novel ligands in  $\beta_1$ AR to find a potential inhibitor for the receptor, which could become a

candidate for new prostate cancer treatments. The interaction energies between these potential inhibitors and the active site were calculated using Density Functional Theory (DFT). The ligands were varied in size, charge, and substituents in order to establish trends within the structures that had strong interaction energies. The positions of the ligands in the active site were optimized using M062X [14], a hybrid DFT method which provides accurate non-bonded interaction energies [15]. The interaction energies of the ligands in this study are compared to the interaction energies of the known partial agonist salbutamol [16], and natural substrates adrenaline, noradrenaline, and dopamine (Fig. 1). Noradrenaline has two phenolic hydroxyl groups in the third and fourth positions of the benzene ring with respect to its ethanolammonium substituent; adrenaline has the same basic structure, except with a secondary ammonium on the substituent with a methyl R group. Salbutamol differs by having a hydroxymethyl in the fourth position and a secondary ammonium with a tertbutyl R group in its substituent. Dopamine has the structure of noradrenaline with the ethanolammonium replaced with ethylammonium. For the purpose of consistency, the carbon on the benzene ring of the ligands that corresponds to the ethylammonium substituent in dopamine is given the first position. Dopamine was used as a baseline, as it is structurally similar (Fig. 1) to adrenaline and noradrenaline, which are known catecholamine agonist ligands of  $\beta$ ARs [16], and it has a stronger interaction energy. For a ligand to be considered an inhibitor, it must exhibit an interaction energy that is comparable to that of dopamine. A major contributing factor to the total interaction energies between the ligands and the active site is the interaction of Asp121 with the ligand, due to its negative charge interacting strongly with the charges on the ligands. The goal of this study is to find ligands which would inhibit  $\beta_1$ AR and can be further studied in  $\beta_2$ AR, to halt exponential prostate tumor growth. Testing novel inhibitors ensures that only the necessary receptors for signaling noradrenaline are inhibited and the production of testosterone and androgens is not affected.

## 2. Computational Methods

The available crystal structure of the  $\beta_2$ AR (PDB ID: 5X7D) is bound to a polyethylene glycol-carboxylic acid derivative of Liu-15, a membrane-permeable allosteric beta-blocker, which exhibits positive cooperativity with inverse agonists and negative cooperativity with agonists [17]. As  $\beta_2$ AR was bound to an antagonist, its active site was blocked rather than activated, as it would be with an agonist. Therefore, the structure of the  $\beta_1$ -adrenergic

receptor ( $\beta_1$ AR) was used as a model of the  $\beta_2$ AR binding site, with a pattern of binding on Chain A offset by approximately eight amino acids in its sequence.

The crystal structure of the  $\beta_1$ AR bound to the partial agonist salbutamol was retrieved from the Protein Data Bank (PDB ID: 2Y04) [16]. The  $\beta_1$ AR active site, defined as any amino acid residues with any atom within three angstroms of the bound ligand, includes Asn310, Asn329, Asp121, Phe201, Phe306, Phe307, Ser211, Ser215, Trp117, Tyr333, and Val122. All amino acid sidechains were either protonated or deprotonated to reflect their behavior at physiological pH.

The ligands tested in this study were based on previous work in the lab [14], [18], [19] and are shown in Figure 1. The LP-suite was created based on the structure of dopamine, with various substituents at the sixth position of the dopamine molecule. The substituents on the LP ligands are: OH, NO<sub>2</sub>, Br, CN, CH=CH<sub>2</sub>, and COOH as well as a cyclic variant (Fig. 1). These substituents were chosen to give a range of electronic effects from electron donating to withdrawing and the derivatives were accessible synthetically or commercially available [20]. The MP, KH, SJ, and PG suites were based on the LP-suite and the DP-suite was based on the MP-suite, PG+1 was based on the PG-suite, and the DS-suite was based on DP-H (as discussed below). These ligands vary by charge, being positive, neutral, and negative. The MP-suite was made neutral by substituting the amine group in the LP ligands with a hydroxyl group (Fig. 1). The KH-suite has a nitrile at the sixth position instead of an amine tail and a proton at the X position of the LP ligands (Fig. 1). The majority of the SJ-suite is of the same general structure (dopamine) as the LP ligands, but with different substituents: NH<sub>3</sub><sup>+</sup>, NH<sub>2</sub>CH<sub>3</sub>, NF<sub>3</sub><sup>+</sup>, and CH<sub>3</sub>, the positive substituents making the ligands have an overall +2 charge. Two of the SJ ligands varied in structure from the LP-suite. The first has a nitro substituent shifted to the fifth position of the catecholic ring. The second ligand has only one hydroxyl group and a (*E*)-2-cyanobut-2-enoate in the para position (Fig. 1). The PG-suite substitutes the amine group in the LP-suite with a carboxyl group, giving it a negative charge, with one carbon linker (Fig.1). The PG+1-suite has an additional carbon linker compared to the structure of the PG-suite. The DP-suite places an amino group at the sixth position and has various substituents at the fifth position. The DS-suite has four varying structures. In the first, the hydroxyl tail was replaced with -COCH<sub>3</sub>. In the second, a carbon linker was added to the amine group and hydroxyl tail was shortened by one carbon. In the third, the amino group of the DP-suite was replaced with an -NF<sub>3</sub>. In the

fourth, the amine group was moved from the sixth to the fifth position. All the DP ligands have a positive charge. Only the LP and MP suites have a cyclic variant, placing the amine tail or hydroxyl tail with a heterocyclic ring. Electrostatic potential surfaces for several of these molecules (the strongest and weakest interacting molecule from each suite) are shown in Figure 2. Overall charge and charge localization can be easily visualized from the images.

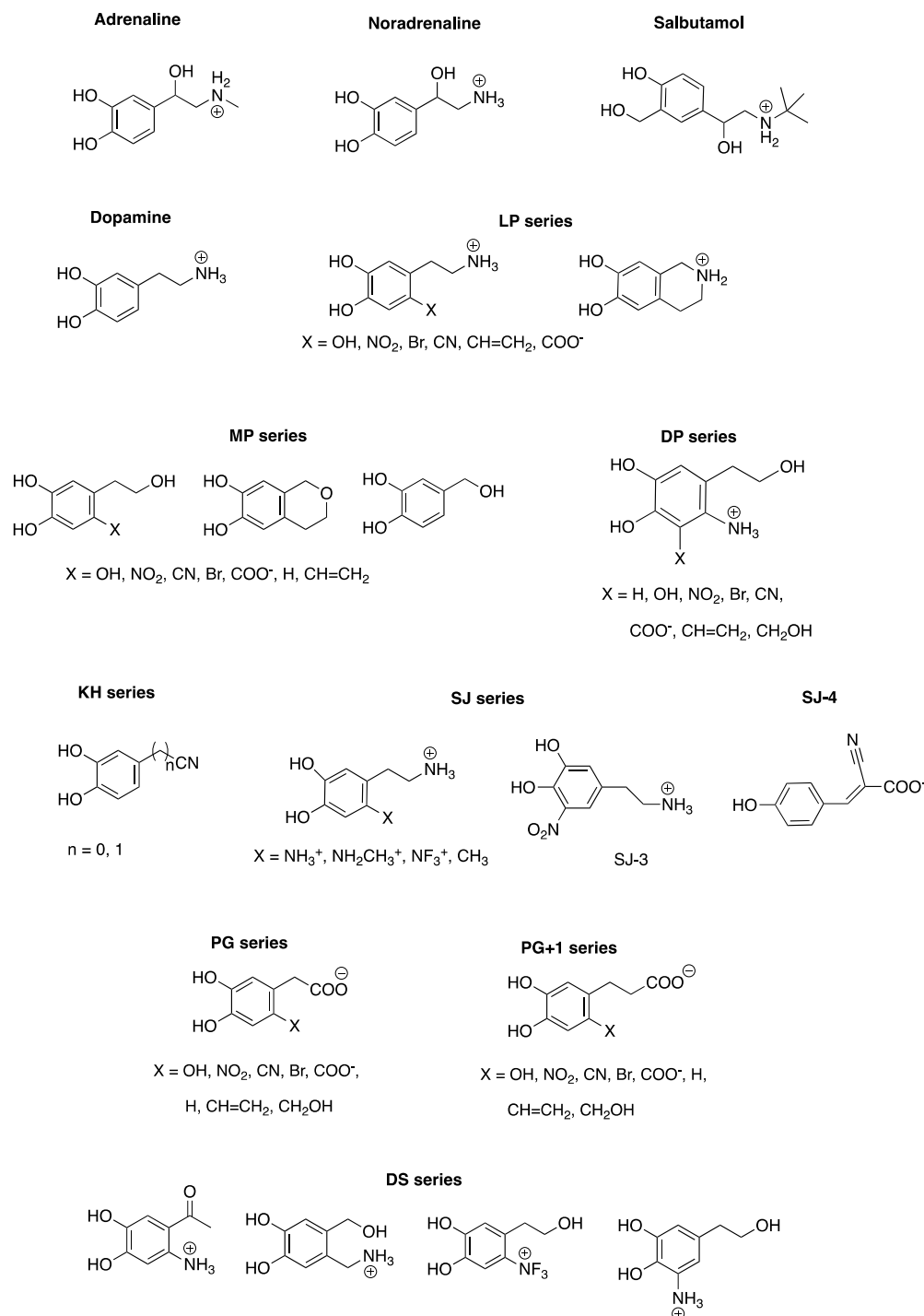


**Figure 1.** Ligands used for study. Structures are protonated/deprotonated to reflect their behavior at physiological pH conditions.

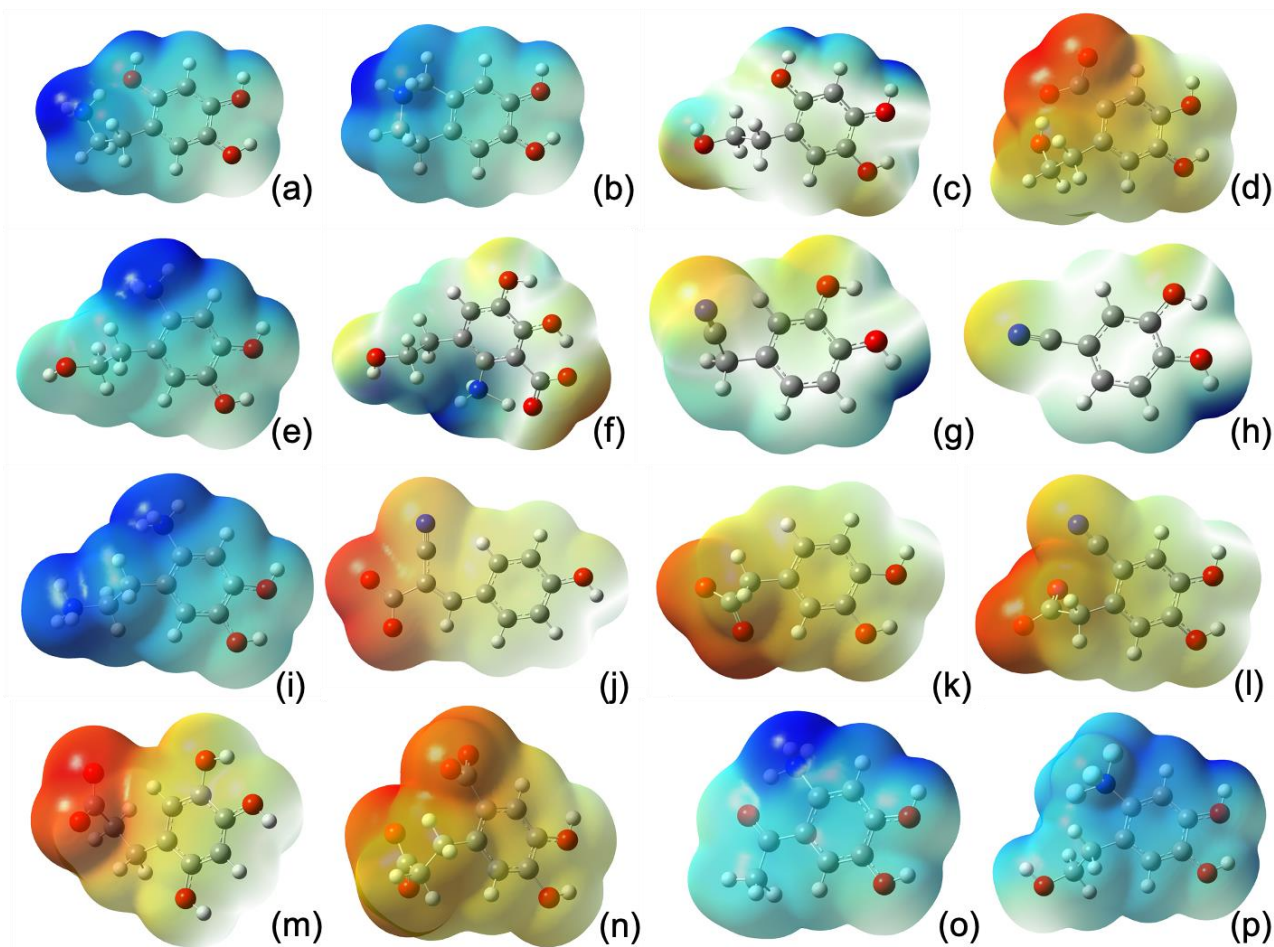


**Figure 2.** Electrostatic surface potentials of the strongest and weakest ligands from each suite. (a) LP-OH, IE = -220.02 kcal/mol. (b) LP Cyclic, IE = -69.25 kcal/mol. (c) MP-OH, IE = -63.04 kcal/mol. (d) MP-COOH, IE = -2.06 kcal/mol. (e) DP-H, IE = -417.65 kcal/mol. (f) DP-COOH, IE = -94.18 kcal/mol. (g) KH+1, IE = -46.75 kcal/mol. (h) KH, IE = -43.80 kcal/mol. (i) SJ-NH<sub>3</sub>, IE = -354.00 kcal/mol. (j) SJ-4, IE = -3.39 kcal/mol. (k) PG-H, IE = -17.21 kcal/mol. (l) PG-CN, IE = 8.13 kcal/mol. (m) PG+1-OH, IE = -17.92 kcal/mol. (n) PG+1-COOH, IE = 24.45 kcal/mol. (o) DS-COCH<sub>3</sub>-6NH<sub>3</sub>, IE = -238.59 kcal/mol. (p) DS-CH<sub>2</sub>CH<sub>2</sub>OH-6NF<sub>3</sub>, IE = -153.71 kcal/mol.

The ligands were placed in the active site in the same starting configuration as salbutamol, which was bound to the  $\beta_1$ AR structure taken from the Protein Data Bank. The positions of all the ligands studied were optimized using the M062X [21] DFT method, with the basis set increased to 6-31G [22]. Relaxed amino acid residue sidechains were implemented to allow for a general rigidity of the active site, but with flexibility in the sidechains. Implicit solvation was used because previous studies have shown that the inclusion of solvation renders more realistic ion stability in the active site and correctly predicts protonation/deprotonation of amino acid sidechains and ligands [23]. The dielectric constant used in this model was 78.3553 and the atomic radius used was from the UFF force field scaled by 1.1 [24]. The counterpoise-corrected energies for the ligands and each amino acid were calculated separately after the ligand positions were optimized, using M062X and the 6-311+G\* basis set. The individual interaction energies were added together to obtain the total interaction energy for the ligand-active site



pair. Amino acids that were bonded by peptide bonds were separated and modified to have a hydroxyl or amine tail to retain neutrality. All calculations were done using Gaussian 16 [24]. For the suites with a general pattern of strong interaction energies (primarily positively charged suites), the ligand with the most favorable interaction is shown in the active site. For the suites with weaker interaction energies (primarily negatively charged suites), the ligand with the least favorable interaction is shown bound in the active site.

### **3. Results and Discussion**

#### **3.1 Natural Inhibitors**

Salbutamol was tested because it is a known partial agonist in the  $\beta_1$ AR [8]. Adrenaline and noradrenaline were tested because they are known catecholamine agonists of  $\beta$ ARs [8]. Dopamine was tested as it is structurally similar to adrenaline and noradrenaline, and it is typically used as the baseline interaction energy for similar research in our group. Therefore, the total interaction energies for these four molecules were used as the baseline for comparison of the functionality of other ligands as potential new inhibitors. The total interaction energy of dopamine (-177.38 kcal/mol) was stronger than that of salbutamol (-67.82 kcal/mol), adrenaline (-129.82 kcal/mol), and noradrenaline (-158.12 kcal/mol) due almost entirely to the strong electrostatic interaction between the positive dopamine and the negative aspartate (Table 1). The interaction energy of dopamine is the minimum interaction energy that would be expected from any new inhibitors that would work well in the active site.

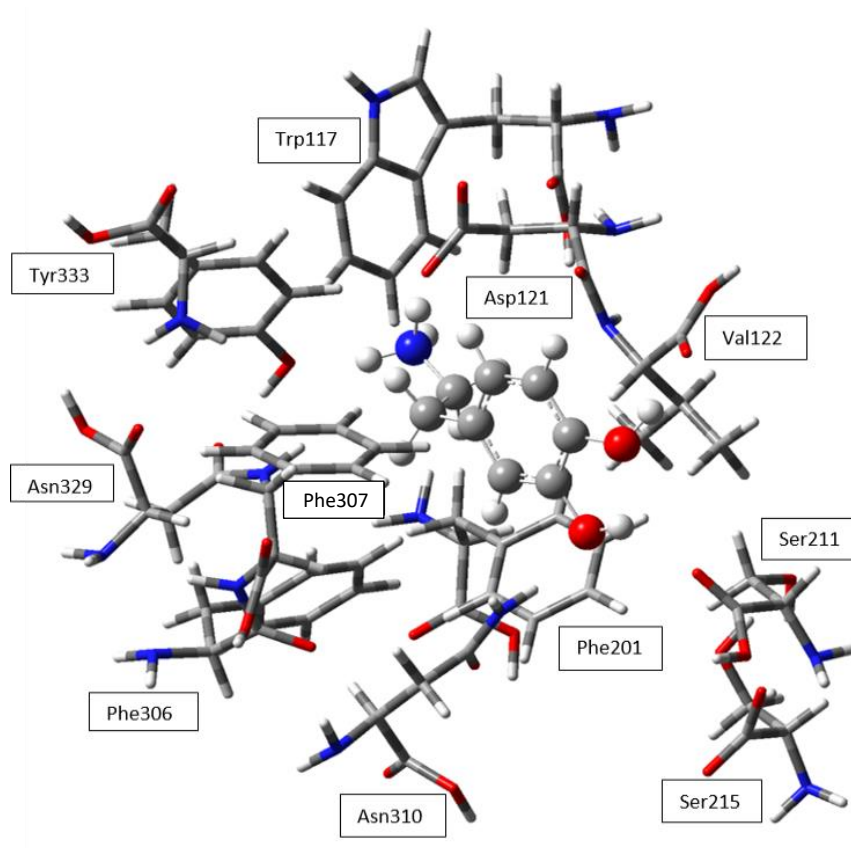


**Figure 2.** Dopamine bound to the  $\beta_1$ AR active site.

**Table 1.** M062X calculations of interaction energies of the M062X optimized natural inhibitors. Energies in kcal/mol.

	ASP121	ASN310	ASN329	PHE201	PHE306	PHE307	SER211	SER215	TRP117	TYR333	VAL122	TOTAL
<i>Salbutamol</i>	-27.29	-5.55	-7.48	-2.35	-0.38	-3.00	-6.18	-0.47	-1.27	-3.03	-10.82	-67.82
<i>Adrenaline</i>	-83.13	-15.11	2.53	-4.49	-3.82	-0.84	-0.92	-0.92	-1.19	-8.91	-13.02	-129.82
<i>Noradrenaline</i>	-86.11	-25.22	2.41	-11.63	-4.32	-2.65	0.28	-6.70	-2.33	-9.24	-12.61	-158.12
<i>Dopamine</i>	-130.66	-3.48	-2.07	-0.78	-3.16	-1.89	-17.14	14.48	-11.50	-4.81	-16.38	-177.38

### 3.2. LP-Suite

The LP-suite (Fig. 1) was the first to be tested. This series of molecules was derived from dopamine with a substituent at the 6-position on the ring and have an overall charge of +1 due to the protonated ammonium tail, except for LP Cyclic and LP-COOH, which is neutral and has a -1 charge, respectively. The interaction energies of this suite ranged from -69.25 kcal/mol to -220.02 kcal/mol (Table 2), which suggests that all of the LP ligands could function as inhibitors in the active site as they are all greater than the interaction energy of salbutamol. LP-OH has the strongest interaction due to the favorable interaction with Asp121 (Fig. 3). The weakest interaction

energies were those of LP Cyclic (-69.25 kcal/mol) and LP-COOH (-87.36). LP Cyclic has the weakest interaction energy due to suboptimal distance of the nitrogen in the ring to Asp121 to have a strong interaction. The weak interaction of LP-COOH is due to the weaker interaction between Asp121 with the ligands due to its negative charge instead of the +1 charge in the rest of the molecules. The rest of the ligands had similar interaction energies, ranging from -192.40 kcal/mol to -220.02 kcal/mol, the highest being that of LP-OH. The interaction energies of the LP-suite, except for LP Cyclic and LP-COOH, are stronger than that of dopamine, which makes them effective potential inhibitors of the  $\beta_2$ AR active site.

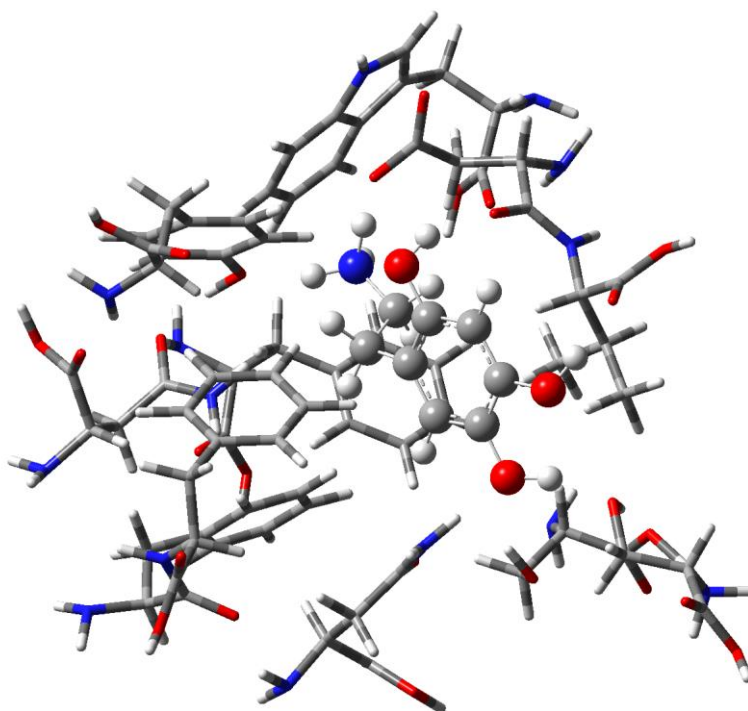


**Figure 3.** LP-OH bound to the  $\beta_1$ AR active site.

**Table 2.** M062X calculations of interaction energies of the M062X optimized LP-suite. Energies in kcal/mol.

	<i>ASP121</i>	<i>ASN310</i>	<i>ASN329</i>	<i>PHE201</i>	<i>PHE306</i>	<i>PHE307</i>	<i>SER211</i>	<i>SER215</i>	<i>TRP117</i>	<i>TYR333</i>	<i>VAL122</i>	<i>TOTAL</i>
<b>LP-OH</b>	-133.73	-6.30	-2.03	-11.81	-3.38	-1.56	-4.18	-10.11	-16.55	-17.01	-23.36	-220.02
<b>LP Cyclic</b>	-3.82	2.11	-7.69	-10.15	-4.66	-3.38	-8.00	4.47	-24.08	-3.03	-11.03	-69.25
<b>LP-NO<sub>2</sub></b>	-117.37	-10.50	-0.51	-13.35	-5.39	-2.67	-60.36	50.31	-9.71	-18.58	-11.89	-200.02
<b>LP-Br</b>	-113.75	-10.32	-1.00	-11.68	-3.89	-1.46	-2.67	-7.15	-8.77	-16.27	-15.44	-192.40
<b>LP-CN</b>	-118.09	-9.61	0.12	-12.51	-4.35	-1.42	-60.01	50.01	-9.28	-16.92	-15.30	-197.37
<b>LP-CH=CH<sub>2</sub></b>	-121.62	-9.44	-1.02	-12.25	-3.84	-1.66	-2.95	-6.34	-9.51	-16.28	-14.95	-199.86
<b>LP-COOH</b>	-33.03	-6.21	-1.63	-6.90	-1.30	-0.56	-54.32	46.05	-4.49	-13.81	-11.15	-87.36

### 3.3. MP-Suite

The MP-suite was based on the LP-suite where the positively charged ammonium was replaced with a neutral hydroxyl group (Fig.1) with the same substituents at the 6-position to investigate the effects of the overall charge on binding and the difference between a polar, uncharged and polar, charged tail. The MP molecules are neutral, except for MP-COOH, which has an overall charge of -1. The interaction energies of the MP-suite ranged from -2.06 kcal/mol to -63.04 kcal/mol (Table 3). The weakest interaction energy was that of MP-COOH (Fig. 4), due to its negative charge, which greatly impacts the interaction energy between the ligand and the negatively charged Asp121, contributing heavily to a more positive overall interaction energy. None of the MP ligands exhibited interaction energies that were more negative than that of dopamine, making them inefficient inhibitors of  $\beta_2$ AR.

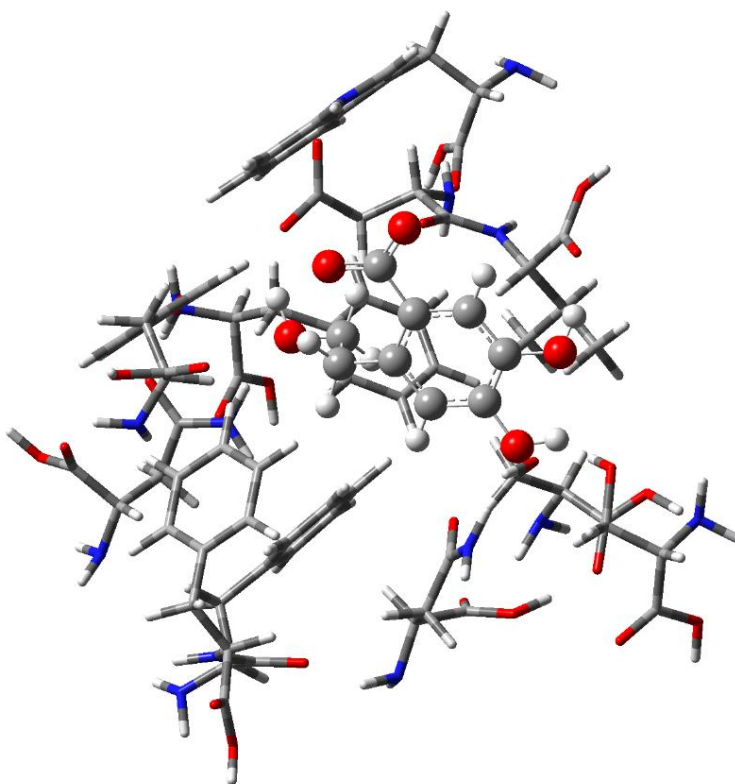


**Figure 4.** MP-COOH bound to the  $\beta_1$ AR active site.

**Table 3.** M062X calculations of interaction energies of the M062X optimized MP-suite. Energies in kcal/mol.

	<i>ASP121</i>	<i>ASN310</i>	<i>ASN329</i>	<i>PHE201</i>	<i>PHE306</i>	<i>PHE307</i>	<i>SER211</i>	<i>SER215</i>	<i>TRP117</i>	<i>TYR333</i>	<i>VAL122</i>	<i>TOTAL</i>
<b>MP-OH</b>	-27.12	-6.46	-5.62	-2.09	0.56	-1.25	-5.13	-2.95	0.04	-2.71	-10.32	-63.04
<b>MP-NO<sub>2</sub></b>	-19.10	-4.90	-5.00	-1.94	0.48	-1.47	-6.24	-3.15	-0.21	-4.27	-12.92	-58.72
<b>MP-CN</b>	-16.85	-5.54	-4.74	-2.17	0.30	-0.95	-5.70	-3.18	-0.69	-3.58	-13.19	-56.29
<b>MP-Br</b>	-19.75	-6.39	-5.21	-2.07	0.53	-1.21	-2.62	-5.69	-0.09	-3.80	-12.43	-58.73

	<i>ASP121</i>	<i>ASN310</i>	<i>ASN329</i>	<i>PHE201</i>	<i>PHE306</i>	<i>PHE307</i>	<i>SER211</i>	<i>SER215</i>	<i>TRP117</i>	<i>TYR333</i>	<i>VAL122</i>	<i>TOTAL</i>
<b>MP-COOH</b>	45.98	-5.36	-9.25	-3.01	1.07	-2.98	-4.95	-3.71	-0.93	-7.90	-11.04	-2.06
<b>MP-H</b>	-23.09	-6.13	-5.31	-2.08	0.46	-1.01	-3.14	-5.03	0.11	-2.72	-11.18	-59.12
<b>MP-CH=CH<sub>2</sub></b>	-21.66	-6.37	-5.81	-2.16	0.45	-1.34	-3.05	-5.25	0.30	-3.91	-11.75	-60.55
<b>MP Cyclic</b>	-8.65	-5.79	-0.11	-1.85	-0.67	-0.36	-3.28	-4.85	-0.25	-3.05	-11.21	-40.08
<b>MP-CH<sub>2</sub>OH</b>	-24.17	-4.78	-5.82	-2.18	0.47	-1.37	-3.60	-5.16	0.13	-3.65	-11.96	-62.09

### 3.4. DP-Suite

The DP-suite was derived from the MP-suite with the addition of a positively charged ammonium group in the sixth position (Fig.1) to investigate the effect of moving the ammonium group that position to maximize interaction with Asp121. The substituent at the fifth position continued to be varied throughout the suite. The overall charge of the molecules is +1, except for DP-COOH, which is neutral. For that reason, it also has the weakest interaction energy out of the DP ligands, -94.18 kcal/mol (Table 4). The interaction energies of the DP-suite ranged from -94.18 kcal/mol to -417.65 kcal/mol (Table 4). The strongest interaction energy was that of DP-H (-417.65 kcal/mol, Fig. 5), which is the strongest interaction energy out of all the ligands in all the suites that have been tested so far. The small substituent and direct binding on the ammonium to the ring leads to less steric hindrance, which allows the ammonium to be positioned more optimally for a strong interaction with Asp121. Even though the DP ligands have a wide range of interaction energies, all but DP-COOH and DP-OH are more negative than the interaction energy of dopamine, which would make them effective as potential inhibitors of the  $\beta_2$ AR active site.

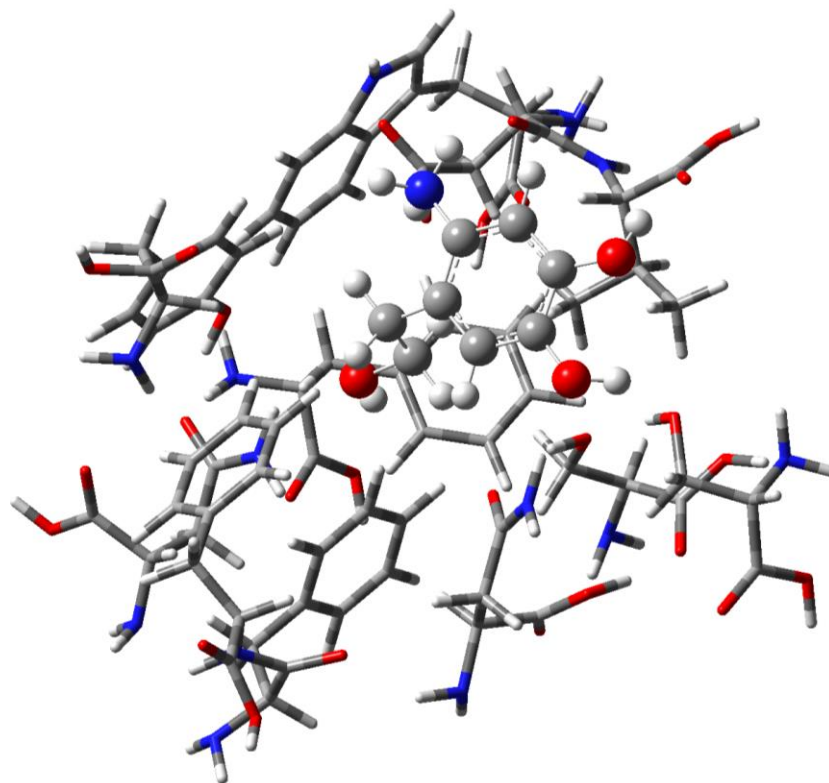


**Figure 5.** DP-H bound to the  $\beta_1$ AR active site.

**Table 4.** M062X calculations of interaction energies of the M062X optimized DP-suite. Energies in kcal/mol.

	<i>ASP121</i>	<i>ASN310</i>	<i>ASN329</i>	<i>PHE201</i>	<i>PHE306</i>	<i>PHE307</i>	<i>SER211</i>	<i>SER215</i>	<i>TRP117</i>	<i>TYR333</i>	<i>VAL122</i>	<i>TOTAL</i>
<b>DP-H</b>	-367.87	-9.82	-2.34	-5.86	-2.56	-1.33	-2.71	-7.98	-0.97	-2.08	-14.13	-417.65
<b>DP-OH</b>	-85.97	-7.14	0.43	-5.90	-2.60	-1.34	-2.66	-8.11	-0.99	-2.23	-13.38	-129.90
<b>DP-NO<sub>2</sub></b>	-206.80	-10.17	-3.91	-2.97	-1.71	-1.04	-2.64	-9.03	-2.12	-8.90	-10.74	-260.02
<b>DP-Br</b>	-187.36	-10.91	-2.02	-5.46	-2.28	-0.91	-2.53	-8.83	-1.20	-2.44	-13.66	-237.60
<b>DP-CN</b>	-149.09	-11.55	-2.06	-5.45	-1.79	-1.04	-2.62	-10.01	-1.15	-2.91	-15.23	-202.89
<b>DP-COOH</b>	-66.90	-7.03	-3.97	-1.74	-0.06	-1.06	-2.53	-5.01	-0.53	-2.78	-2.58	-94.18
<b>DP-CH=CH<sub>2</sub></b>	-130.39	-10.16	-2.20	-5.23	-2.01	-0.95	-2.48	-8.38	-0.47	-2.28	-15.69	-180.22
<b>DP-CH<sub>2</sub>OH</b>	-130.68	-7.38	-2.10	-2.77	-2.10	-1.19	-2.21	-8.65	0.95	-6.40	-17.35	-179.87

### 3.5. KH-Suite

The KH-suite was based on the LP-suite, where the positively charged ammonium was replaced with a neutral nitrile with the nitrile group attached directly to the ring or separated by a methylene group; no other substituent on the ring besides the two hydroxyl groups (Fig. 1). The overall charge of the KH molecules is neutral, and the number of carbons in the carbon chain (n) was either 0 or 1. The interaction energies of the KH ligands were more

positive than that of dopamine, making them ineffective inhibitors of the  $\beta_2$ AR active site. As can be seen in Figure 6, these ligands are unable to interact with Asp121, which has been a major contributor to the interaction energies in previous suites.

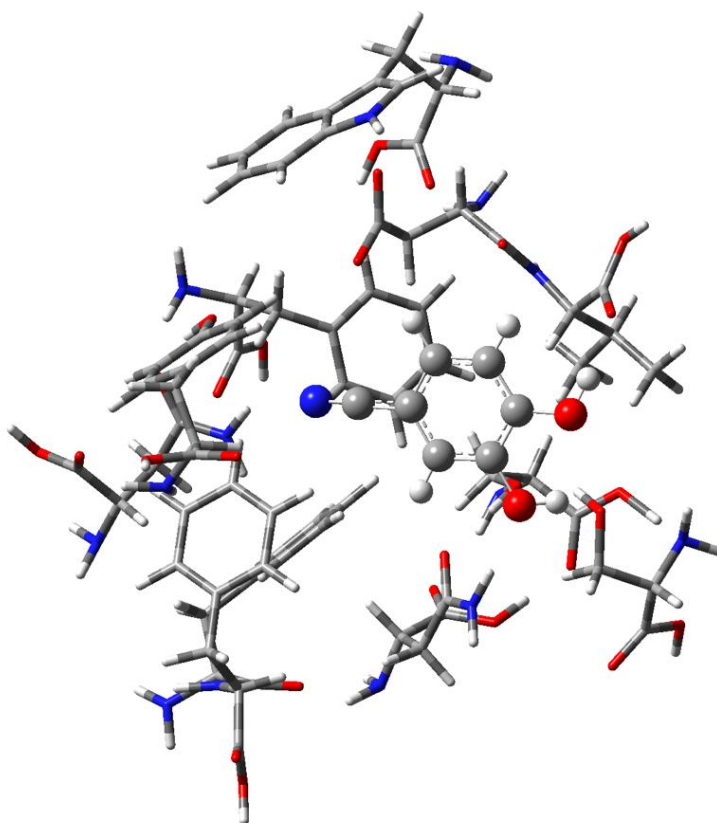


**Figure 6.** KH bound to the  $\beta_1$ AR active site.

**Table 5.** M062X calculations of interaction energies of the M062X optimized KH-suite. Energies in kcal/mol.

	<i>ASP121</i>	<i>ASN310</i>	<i>ASN329</i>	<i>PHE201</i>	<i>PHE306</i>	<i>PHE307</i>	<i>SER211</i>	<i>SER215</i>	<i>TRP117</i>	<i>TYR333</i>	<i>VAL122</i>	<i>TOTAL</i>
<b>KH (n=0)</b>	-12.89	-5.84	-4.05	-0.77	0.42	-1.02	-3.01	-5.81	0.33	-0.02	-11.14	-43.80
<b>KH+1 (n=1)</b>	-17.34	-4.31	-4.25	-0.62	0.17	-0.34	-3.04	-5.74	0.66	-0.72	-11.21	-46.75

### 3.6. SJ-Suite

The SJ-suite was based on the LP-suite. SJ-CH<sub>3</sub>, SJ-NF<sub>3</sub>, SJ-NH<sub>2</sub>CH<sub>3</sub>, and SJ-NH<sub>3</sub> have the same general structure as the LP molecules, but have different substituents at the sixth position. The SJ-3 molecule also has the same general structure as the LP molecules and has a nitro group at the fifth position. The SJ-4 molecule has one hydroxyl group and CH=C(CN)COOH in the *para* position. The overall charge of the SJ-NF<sub>3</sub>, SJ-NH<sub>2</sub>CH<sub>3</sub>, and SJ-NH<sub>3</sub> ligands is +2, the overall charge of SJ-3 and SJ-CH<sub>3</sub> is +1, and SJ-4 has an overall charge of -1. This suite of molecules was created specifically to interact well with the MAOB enzyme [25]. The molecular suites used in

this work will bind more or less strongly to the MAOB active site, which may then affect the metabolism of dopamine and other catechols. Likewise, molecules created to interact well with MAOB may interact strongly with the  $\beta_1$ AR active site, and so all molecules created by our group are analyzed in all relevant active sites to test for selectivity. Substituents with a positive charge in which an electronegative atom is directly attached to an aromatic ring (such as  $-\text{NF}_3^+$  and  $-\text{NH}_3^+$  in this suite), the overall effect is significantly electron withdrawing. This creates greater charge polarization and stronger interaction with charged residues in the active site. The interaction energies of the SJ-suite range from -3.39 kcal/mol to -354.00 kcal/mol (Table 6). The weakest interaction energy was that of SJ-4, due to the negative charge. SJ-NH<sub>3</sub> (Fig. 7) is the ligand with the second strongest interaction energy from all the ligands that have been tested so far (-354.00 kcal/mol). The other SJ ligands with +2 charges also exhibited strong interaction energies. However, they were not as strong as DP-H (-417.65 kcal/mol, Table 4), due to the electrostatic and hydrogen bonding between the deprotonated carboxyl group on Asp121 and the hydrogens on the amine groups. Having two positive charges on the ligand makes the interaction with Asp121 weaker because it is dispersed between the two ammonium groups. All the SJ ligands, with the exception of SJ-4, would effectively inhibit the active site.



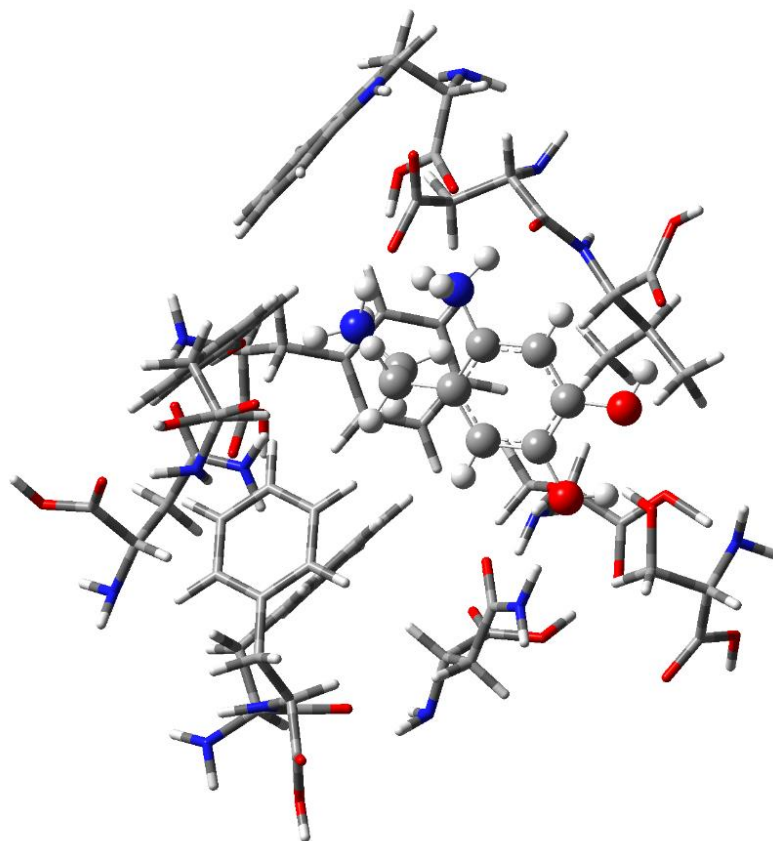


**Figure 7.** SJ-NH<sub>3</sub> bound to the  $\beta_1$ AR active site.

**Table 6.** M062X calculations of interaction energies of the M062X optimized SJ-suite. Energies in kcal/mol.

	<i>ASP121</i>	<i>ASN310</i>	<i>ASN329</i>	<i>PHE201</i>	<i>PHE306</i>	<i>PHE307</i>	<i>SER211</i>	<i>SER215</i>	<i>TRP117</i>	<i>TYR333</i>	<i>VAL122</i>	<i>TOTAL</i>
<b>SJ-3</b>	-126.06	-10.76	-0.91	-12.34	-5.36	-1.89	-2.80	-7.30	-12.36	-17.12	-8.92	-205.82
<b>SJ-4</b>	42.13	-2.49	-12.90	-11.15	-1.95	-3.66	-4.27	-0.63	-1.54	5.07	-12.00	-3.39
<b>SJ-CH<sub>3</sub></b>	-123.14	-11.01	-0.26	-10.95	-4.60	-2.19	-2.72	-6.37	-3.51	-16.63	-12.56	-194.15
<b>SJ-NF<sub>3</sub></b>	-206.25	-14.23	-0.92	-17.81	-8.74	-4.30	-4.08	-14.77	-9.87	-23.83	-20.83	-325.63
<b>SJ-NH<sub>2</sub>CH<sub>3</sub></b>	-232.15	-11.82	-2.05	-18.22	-7.90	-3.61	-3.45	-10.38	-16.53	-24.08	-18.17	-348.36
<b>SJ-NH<sub>3</sub></b>	-236.96	-12.94	-2.34	-18.39	-8.25	-3.86	-3.69	-10.81	-14.95	-23.79	-18.01	-354.00

### 3.7. PG-Suite

The PG-suite was based on the LP-suite where the tail was shortened and the positively charged ammonium was replaced with a negatively charged carboxyl group (deprotonated under physiological conditions) (Fig. 1). This suite was designed to examine the effect of a different overall charge. Excluding PG-COOH, which has an overall charge of -2, the PG molecules have an overall charge of -1. This suite was tested to confirm that negatively charged ligands do not have strong interaction energies and would not be suitable to serve as inhibitors. The

interaction energies range from 8.13 kcal/mol to -17.21 kcal/mol (Table 7). PG-H had the strongest interaction energy of -17.21 kcal/mol, possibly due to having the least steric hindrance in the active site and the least repulsion with Asp121. PG-CN and PG-COOH had the weakest interaction energies, 8.13 kcal/mol and 6.76 kcal (Table 7), respectively. None of the ligands had interaction energies negative enough to be effective inhibitors of  $\beta_2$ AR.

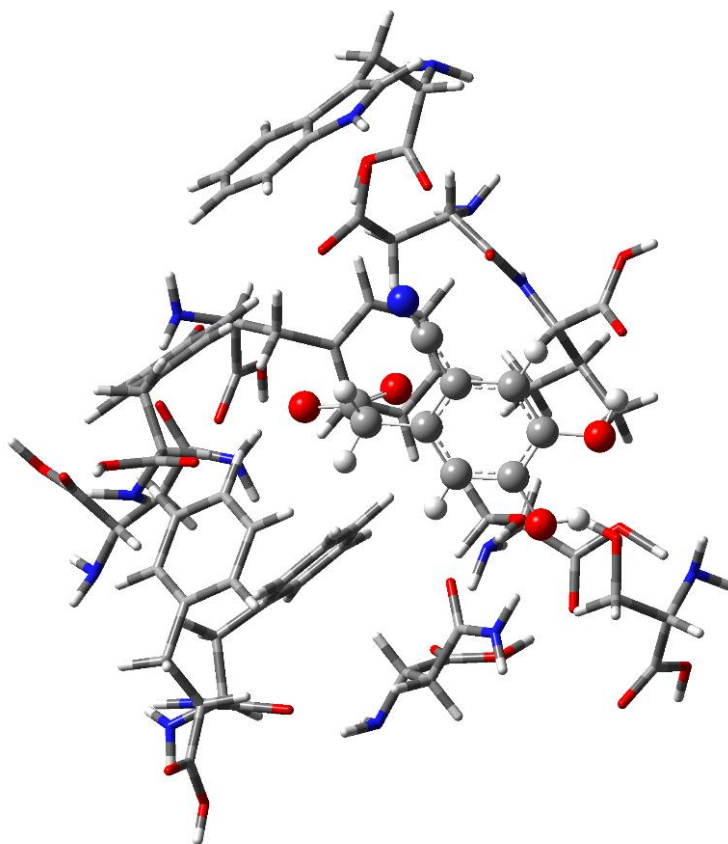


**Figure 8.** PG-CN bound to the  $\beta_1$ AR active site.

**Table 7.** M062X calculations of interaction energies of the M062X optimized PG-suite. Energies in kcal/mol.

	<i>ASP121</i>	<i>ASN310</i>	<i>ASN329</i>	<i>PHE201</i>	<i>PHE306</i>	<i>PHE307</i>	<i>SER211</i>	<i>SER215</i>	<i>TRP117</i>	<i>TYR333</i>	<i>VAL122</i>	<i>TOTAL</i>
<b>PG-OH</b>	39.88	-2.45	-17.91	-3.40	-1.87	-5.06	-5.31	-4.53	1.30	-2.91	-13.13	-15.38
<b>PG-NO<sub>2</sub></b>	47.22	-2.37	-14.88	-6.73	0.37	-3.42	-5.00	-4.38	1.12	-5.44	-15.80	-9.29
<b>PG-CN</b>	63.03	-1.51	-16.42	-2.94	-1.65	-4.72	-5.37	-5.00	0.08	-2.62	-14.75	8.13
<b>PG-Br</b>	45.32	-2.96	-16.61	-5.98	0.80	-3.21	-4.62	-4.65	2.04	-3.95	-14.40	-8.21
<b>PG-COOH</b>	101.85	-1.88	-22.73	-13.74	-3.71	-8.53	-8.04	-3.65	-0.05	-15.94	-16.81	6.76
<b>PG-H</b>	40.80	-1.89	-18.25	-2.66	-3.09	-4.89	-5.88	-4.86	1.34	-3.44	-14.37	-17.21
<b>PG-CH=CH<sub>2</sub></b>	54.70	-1.66	-19.27	-11.59	-3.26	-4.96	-5.55	-4.67	0.11	-3.69	-12.63	-12.49
<b>PG-CH<sub>2</sub>OH</b>	52.05	-2.28	-17.55	-6.11	-0.81	-5.37	-5.38	-4.50	0.53	-3.74	-14.35	-7.51

### 3.8. PG+1-Suite

The PG+1-suite was based on the PG-suite, altering the tail by extending the carbon chain by one carbon (Fig. 1). As in the PG-suite, the PG+1 molecules have an overall charge of -1, with the exception of PG1-COOH, which has a charge of -2. The interaction energies range from 24.45 kcal/mol to -19.67 kcal/mol (Table 8). PG1-CH=CH<sub>2</sub> showed had the strongest interaction, and not surprisingly, PG1-COOH, with the -2 overall charge, had the weakest interaction energies, 24.45 kcal (Table 8), due to the repulsion between the ligand and Asp121. Just like in the PG-suite, none of the ligands had interaction energies negative enough to be effective inhibitors of  $\beta_2$ AR.

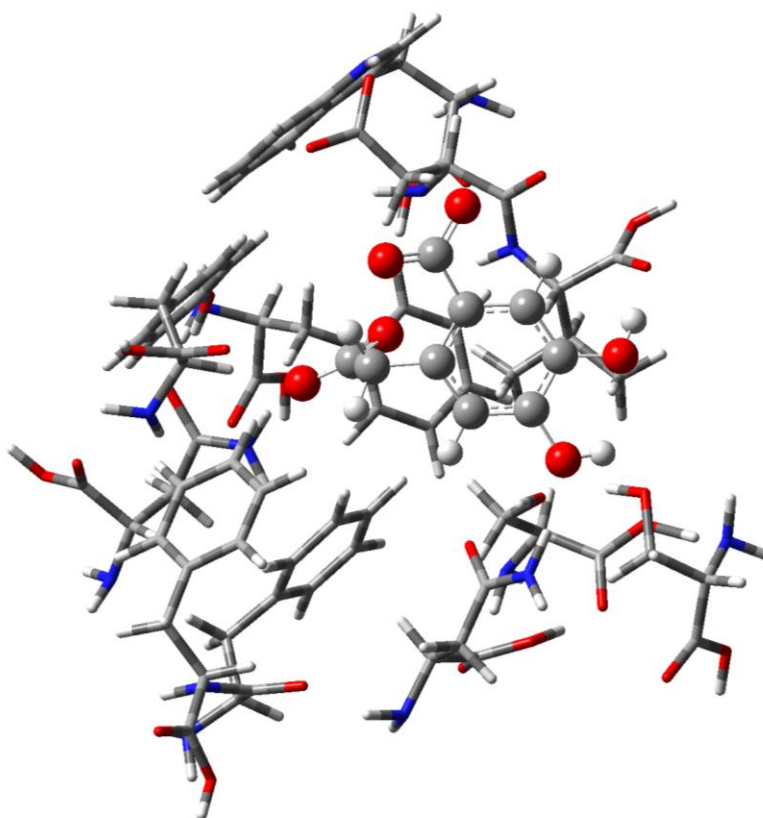


**Figure 9.** PG1-COOH bound to the  $\beta_1$ AR active site.

**Table 8.** M062X calculations of interaction energies of the M062X optimized PG+1-suite. Energies in kcal/mol.

	<i>ASP121</i>	<i>ASN310</i>	<i>ASN329</i>	<i>PHE201</i>	<i>PHE306</i>	<i>PHE307</i>	<i>SER211</i>	<i>SER215</i>	<i>TRP117</i>	<i>TYR333</i>	<i>VAL122</i>	<i>TOTAL</i>
<b>PG1-OH</b>	26.71	-4.06	-1.76	-4.13	0.27	-2.54	-4.74	-4.35	6.37	-5.09	-24.60	-17.92
<b>PG1-NO<sub>2</sub></b>	61.15	-3.69	-0.81	-7.79	0.46	-2.32	-3.96	-4.36	3.81	-5.68	-18.54	18.27
<b>PG1-CN</b>	46.20	-3.23	-1.11	-6.28	-0.04	-1.81	-4.35	-4.55	2.90	-5.62	-18.50	3.61
<b>PG1-Br</b>	51.13	-3.31	-1.17	-4.45	-0.00	-2.06	-4.60	-4.29	3.51	-5.40	-16.89	12.47
<b>PG1-COOH</b>	109.07	-2.34	-23.84	-8.09	-3.47	-10.55	-7.31	-3.68	-0.29	-7.34	-17.70	24.45

	<i>ASP121</i>	<i>ASN310</i>	<i>ASN329</i>	<i>PHE201</i>	<i>PHE306</i>	<i>PHE307</i>	<i>SER211</i>	<i>SER215</i>	<i>TRP117</i>	<i>TYR333</i>	<i>VAL122</i>	<i>TOTAL</i>
<b>PG1-H</b>	52.20	-3.63	-1.38	-2.41	0.18	-2.38	-4.92	-4.00	3.01	-5.64	-15.15	15.86
<b>PG1-CH=CH<sub>2</sub></b>	48.51	-3.40	-21.04	-5.48	0.62	-1.90	-8.08	-5.12	0.53	-8.45	-15.86	-19.67
<b>PG1-CH<sub>2</sub>OH</b>	53.04	-3.09	-18.96	-7.48	-1.16	-8.75	-4.78	-4.43	-0.30	-2.91	-12.59	-11.42

### 3.9. DS-Suite

The DS-suite was designed especially for  $\beta_1$ AR and therefore, was based on the DP-H molecule, as it has the most negative interaction energy. The ligands in this suite had a variety of modifications in an attempt to maximize interactions with the receptor and see what would be tolerated. In the DS-CH<sub>2</sub>OH-6CH<sub>2</sub>NH<sub>3</sub> ligand, the hydroxyl carbon chain was shortened by one and the amine carbon chain was shortened by one. In the DS-CH<sub>2</sub>CH<sub>2</sub>OH-5NH<sub>3</sub> ligand, the amine was shifted from the sixth to the fifth position (Fig. 1). In the DS-COCH<sub>3</sub>-6NH<sub>3</sub> ligand, the hydroxyl group was replaced with a ketone (Fig. 1). In the DS-CH<sub>2</sub>CH<sub>2</sub>OH-6NF<sub>3</sub> ligand, the amine was replaced with nitrogen trifluoride (Fig. 1). All the ligands in the DS-suite have an overall +1 charge. The interaction energies of this suite ranged from -162.37 kcal/mol to -238.59 kcal/mol (Table 9). Replacing the hydroxyl group with a ketone in DS-COCH<sub>3</sub>-6NH<sub>3</sub> (Fig. 10) resulted in an interaction energy of -238.59 kcal/mol (Table 9), which was the strongest interaction energy within the DS-suite, but significantly weaker than the interaction energy of the DP-H molecule (-417.65 kcal/mol, Table 4). It can be seen that the interaction energy is strongest when the ammonium group is directly attached to the ring in the sixth position. Substituting the ammonium for a nitrogen trifluoride in DS-CH<sub>2</sub>CH<sub>2</sub>OH-6NF<sub>3</sub> (as compared to DP-H) had a negative effect on the interaction energy despite its positive charge. Moving the ammonium to the fifth position in DS-CH<sub>2</sub>CH<sub>2</sub>OH-5NH<sub>3</sub> also weakened the interaction energy as compared to when it is in the sixth position in DP-H. DS-COCH<sub>3</sub>-6NH<sub>3</sub> is the only ligand from the DS-suite with a strong enough interaction energy to be an effective potential inhibitor of  $\beta_2$ AR.

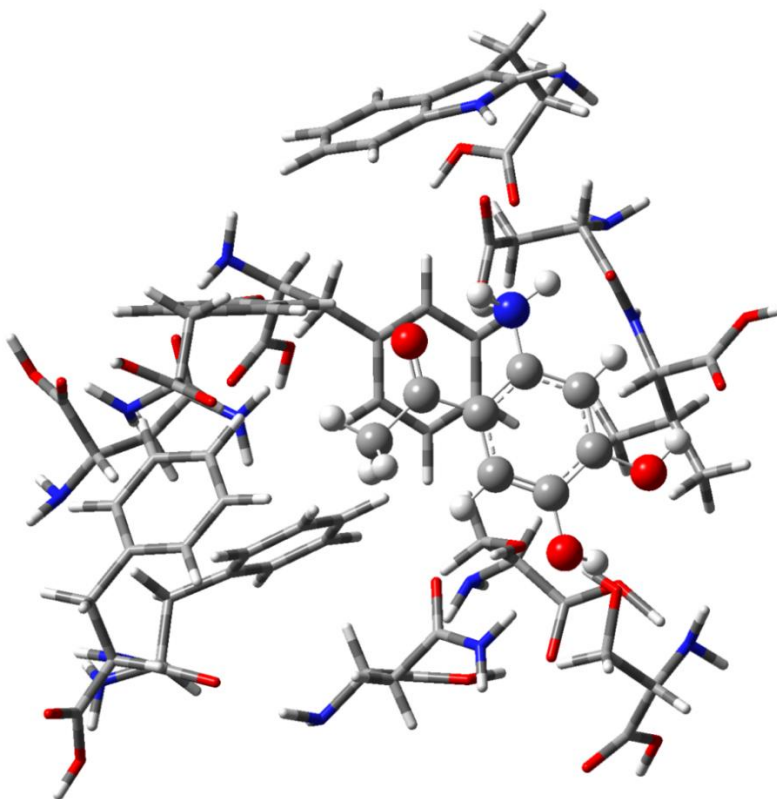


**Figure 10.** DS-COCH<sub>3</sub>-6NH<sub>3</sub> bound to the  $\beta_1$ AR active site.

**Table 9.** M062X calculations of interaction energies of the M062X optimized DS-suite. Energies in kcal/mol.

	<i>ASP121</i>	<i>ASN310</i>	<i>ASN329</i>	<i>PHE201</i>	<i>PHE306</i>	<i>PHE307</i>	<i>SER211</i>	<i>SER215</i>	<i>TRP117</i>	<i>TYR333</i>	<i>VAL122</i>	<i>TOTAL</i>
DS-CH <sub>2</sub> OH- 6CH <sub>2</sub> NH <sub>3</sub>	-115.12	-4.32	-4.25	-7.16	-2.22	-0.35	-2.39	-9.28	-2.19	-9.73	-12.29	-169.31
DS-CH <sub>2</sub> CH <sub>2</sub> OH- 5NH <sub>3</sub>	-104.66	-7.52	-2.32	-2.60	-1.37	-1.06	-3.27	-9.41	-0.10	-4.83	-25.26	-162.37
DS-COCH <sub>3</sub> -6NH <sub>3</sub>	-197.21	-7.65	1.23	-1.13	-1.29	-0.39	-2.60	-9.37	0.04	-3.89	-16.31	-238.59
DS-CH <sub>2</sub> CH <sub>2</sub> OH-6NF <sub>3</sub>	-99.99	-7.62	-1.26	-2.98	-2.10	-1.57	-2.97	-11.06	-0.79	-5.99	-17.39	-153.71

#### 4. Conclusion

If the ligands tested in this study are able to inhibit  $\beta_2$ AR, it would slow down prostate tumor growth, which could be explored as an alternative to chemotherapy for cancer treatment and a method to prevent cancer progression to CRPC. Overall, it was established that positively charged ligands generally have stronger interaction energies as compared to neutral and negative ligands due to the aspartate at the back of the active site. Neutral and negatively charged ligands do not bind well to the  $\beta_1$ AR. The negatively charged ligands are

repulsed by the negatively charged aspartate and the neutral ligands do not have a strong enough interaction. On the contrary, the negatively charged aspartate interacts with the positive charges on the ligands; the strength of this interaction influences the total interaction energies most. Ligands with less steric hindrance which are able to position the positively charged group more optimally for an interaction with Asp121 also tend to have better interaction energies with the  $\beta_1$ AR active site. The interaction energies are stronger when the positively charged group is bonded directly to the ring, as seen with DP-H, SJ-NH<sub>3</sub>, SJ-NH<sub>2</sub>CH<sub>3</sub>, SJ-NF<sub>3</sub>, and the trend seen in the DS-suite. The sixth position on the benzene is shown to be the optimal position for the ammonium group; the interaction energy is weakened by moving the ammonium to the fifth position as seen in DS-CH<sub>2</sub>CH<sub>2</sub>OH-5NH<sub>3</sub>.

The LP- (with the exception of LP-COOH and LP Cyclic), DP- (with the exception of DP-COOH and DP-OH), SJ- (with the exception of SJ-4) suites and DS-COCH<sub>3</sub>-6NH<sub>3</sub> show promising results to be efficient inhibitors of  $\beta_2$ AR. As  $\beta_1$ AR was used as a model for the  $\beta_2$ AR active site in this study, future work involves comparing the selectivity of the  $\beta_1$ AR versus the  $\beta_2$ AR active sites to determine if these ligands would act as effective inhibitors in both sites. The molecules which, based on the DFT study, qualify as potential inhibitors will be synthesized and tested in assays and that work will be presented in a future communication.

## Acknowledgements

This work was supported by the National Science Foundation ([CHE-1626238](#)).

## References

- [1] R. Siegel, J. Ma, Z. Zou, and A. Jemal, "Cancer statistics, 2014," *CA. Cancer J. Clin.*, vol. 64, no. 1, pp. 9–29, 2014, doi: <https://doi.org/10.3322/caac.21208>.
- [2] G. Kulik, "ADRB2-Targeting Therapies for Prostate Cancer," *Cancers*, vol. 11, no. 3, Mar. 2019, doi: 10.3390/cancers11030358.
- [3] T. M. S. Amaral, D. Macedo, I. Fernandes, and L. Costa, "Castration-Resistant Prostate Cancer: Mechanisms, Targets, and Treatment," *Prostate Cancer*, vol. 2012, pp. 1–11, 2012, doi: 10.1155/2012/327253.
- [4] "Prostate cancer progression after androgen deprivation therapy: mechanisms of castrate resistance and novel therapeutic approaches | Oncogene." <https://www.nature.com/articles/onc2013206#article-info> (accessed Jan. 20, 2021).
- [5] A. H. Zahalka *et al.*, "Adrenergic nerves activate an angio-metabolic switch in prostate cancer," *Science*, vol. 358, no. 6361, pp. 321–326, Oct. 2017, doi: 10.1126/science.aah5072.
- [6] C. Hwang and E. I. Heath, "Angiogenesis inhibitors in the treatment of prostate cancer," *J. Hematol. Oncol. J Hematol Oncol*, vol. 3, no. 1, p. 26, Aug. 2010, doi: 10.1186/1756-8722-3-26.
- [7] P. R. Braadland, H. Ramberg, H. H. Grytli, and K. A. Taskén, "β-Adrenergic Receptor Signaling in Prostate Cancer," *Front. Oncol.*, vol. 4, Jan. 2015, doi: 10.3389/fonc.2014.00375.
- [8] Y. Zhao and W. Li, "Beta-adrenergic signaling on neuroendocrine differentiation, angiogenesis, and metastasis in prostate cancer progression," *Asian J. Androl.*, vol. 21, no. 3, pp. 253–259, 2019, doi: 10.4103/aja.aja\_32\_18.
- [9] N. Shah and M. Brown, "The Sly Oncogene: FOXA1 Mutations in Prostate Cancer," *Cancer Cell*, vol. 36, no. 2, pp. 119–121, Aug. 2019, doi: 10.1016/j.ccell.2019.07.005.
- [10] S. Lehrer and P. H. Rheinstein, "The ADRB1 (Adrenoceptor Beta 1) and ADRB2 Genes Significantly Co-express with Commonly Mutated Genes in Prostate Cancer," *Discov. Med.*, Dec. 2020, Accessed: Jan. 28, 2021. [Online]. Available: <https://www.discoverymedicine.com/Steven-Lehrer/2020/12/adrb1-adrenoceptor-beta-1-adrb2-co-express-in-prostate-cancer/>.
- [11] P. Zhang, X. He, J. Tan, X. Zhou, and L. Zou, "β-arrestin2 mediates β-2 adrenergic receptor signaling inducing prostate cancer cell progression," *Oncol. Rep.*, vol. 26, no. 6, pp. 1471–1477, Dec. 2011, doi: 10.3892/or.2011.1417.
- [12] H. C. S. Chan, S. Filipek, and S. Yuan, "The Principles of Ligand Specificity on beta-2-adrenergic receptor," *Sci. Rep.*, vol. 6, Oct. 2016, doi: 10.1038/srep34736.
- [13] J. G. Baker, "The selectivity of β-adrenoceptor antagonists at the human β1, β2 and β3 adrenoceptors," *Br. J. Pharmacol.*, vol. 144, no. 3, pp. 317–322, Feb. 2005, doi: 10.1038/sj.bjp.0706048.
- [14] R. Evans, L. Peterson, and M. Cafiero, "Evaluation of hybrid and pure DFT methods for the binding of novel ligands in the tyrosine hydroxylase enzyme," *Comput. Theor. Chem.*, vol. 1140, pp. 145–151, Sep. 2018, doi: 10.1016/j.comptc.2018.08.009.
- [15] "Assessment of the Performance of the M05–2X and M06–2X Exchange-Correlation Functionals for Noncovalent Interactions in Biomolecules | Journal of Chemical Theory and Computation." <https://pubs.acs.org/doi/10.1021/ct800308k> (accessed Oct. 06, 2020).
- [16] T. Warne *et al.*, "The structural basis for agonist and partial agonist action on a β 1 -adrenergic receptor," *Nature*, vol. 469, no. 7329, Art. no. 7329, Jan. 2011, doi: 10.1038/nature09746.
- [17] X. Liu *et al.*, "Mechanism of intracellular allosteric β 2 AR antagonist revealed by X-ray crystal structure," *Nature*, vol. 548, no. 7668, Art. no. 7668, Aug. 2017, doi: 10.1038/nature23652.
- [18] A. K. Hatstat, M. Morris, L. W. Peterson, and M. Cafiero, "Ab initio study of electronic interaction energies and desolvation energies for dopaminergic ligands in the catechol-O-methyltransferase active site," *Comput. Theor. Chem.*, vol. 1078, pp. 146–162, Feb. 2016, doi: 10.1016/j.comptc.2016.01.003.
- [19] M. C. Perchik, L. W. Peterson, and M. Cafiero, "The effects of ligand deprotonation on the binding selectivity of the phenylalanine hydroxylase active site," *Comput. Theor. Chem.*, vol. 1153, pp. 19–24, Apr. 2019, doi: 10.1016/j.comptc.2019.02.015.
- [20] J. C. Rote *et al.*, "Catechol reactivity: Synthesis of dopamine derivatives substituted at the 6-position," *Synth. Commun.*, vol. 47, no. 5, pp. 435–441, Mar. 2017, doi: 10.1080/00397911.2016.1269350.
- [21] Y. Zhao and D. G. Truhlar, "The M06 suite of density functionals for main group thermochemistry, thermochemical kinetics, noncovalent interactions, excited states, and transition elements: two new functionals

- and systematic testing of four M06-class functionals and 12 other functionals,” *Theor. Chem. Acc.*, vol. 120, no. 1, pp. 215–241, May 2008, doi: 10.1007/s00214-007-0310-x.
- [22] J.-P. Blaudeau, M. P. McGrath, L. A. Curtiss, and L. Radom, “Extension of Gaussian-2 (G2) theory to molecules containing third-row atoms K and Ca,” *J. Chem. Phys.*, vol. 107, no. 13, pp. 5016–5021, Oct. 1997, doi: 10.1063/1.474865.
- [23] D. J. Bigler, L. W. Peterson, and M. Cafiero, “Effects of implicit solvent and relaxed amino acid side chains on the MP2 and DFT calculations of ligand–protein structure and electronic interaction energies of dopaminergic ligands in the SULT1A3 enzyme active site,” *Comput. Theor. Chem.*, vol. 1051, pp. 79–92, Jan. 2015, doi: 10.1016/j.comptc.2014.10.031.
- [24] M. J. Frisch *et al.*, “Gaussian Inc, Wallingford CT, 2016,” *Gaussian16 Revis. B01*.
- [25] “R. Ancar, S. Jelinek, A. Woody, M. Morris, L. W. Peterson and M. Cafiero, Manuscript in progress.” .